RESEARCH ARTICLE

Cytological behaviour of floral organs and *in silico* characterization of differentially expressed transcript-derived fragments associated with 'floral bud distortion' in soybean

PRASHANT B. KALE[1], PRAVIN V. JADHAV[1]*, RACHANA S. WAKEKAR[1], M. P. MOHARIL[1], A. G. DESHMUKH[2], M. S. DUDHARE[3], R. S. NANDANWAR[4], S. S. MANE[5], J. G. MANJAYA[6] and R. G. DANI[1]

[1]*Biotechnology Centre,* [2]*Nagarjuna Medicinal Garden,* [4]*Department of Agricultural Botany, and* [5]*Department of Plant Pathology, Post Graduate Institute, Dr Panjabrao Deshmukh Krishi Vidyapeeth, Akola 444 104, India*
[3]*Vasantrao Naik College of Agricultural Biotechnology, Dr Panjabrao Deshmukh Krishi Vidyapeeth, Yavatmal 445 001, India*
[6]*Nuclear Agriculture and Biotechnology Division, Bhabha Atomic Research Centre (BARC), Trombay, Mumbai 400 085, India*

Abstract

An attempt was made to understand the 'floral bud distortion' (FBD), an unexplored disorder prevailing in soybean. Cytological behaviour of floral reproductive organs and *in silico* characterization of differentially expressed transcript-derived fragments (TDFs) in symptomatic and asymptomatic soybean plants were carried out. Pollens in asymptomatic plants do not have defects in number, size, shape and function. However, in symptomatic plant, pollens were found nonviable, abnormal in shape and with reduced germination ability. Here, we employed a computational approach, exploring invaluable resources. The tissue-specific transcript profile of symptomatic and asymptomatic sources was compared to determine differentially expressed TDFs associated with FBD to improve its basic understanding. A total of 60 decamer primers produced 197 scorable amplicons, ranged 162–1130 bp, of which 171 were monomorphic and 26 were differentially regulated. Reproducible TDFs were sequenced and characterized for their homology analysis, annotation, protein–protein interaction, subcellular localization and their physical mapping. Homology-based annotation of TDFs in soybean revealed presence of two characterized and seven uncharacterized hits. Annotation of characterized sequences showed presence of genes, namely auxin response factor 9 (ARF9) and forkhead-associated (FHA) domain, which are directly involved in plant development through various pathways, such as hormonal regulation, plant morphology, embryogenesis and DNA repair.

[Kale P. B., Jadhav P. V., Wakekar R. S., Moharil M. P., Deshmukh A. G., Dudhare M. S., Nandanwar R. S., Mane S. S., Manjaya J. G. and Dani R. G. 2016 Cytological behaviour of floral organs and *in silico* characterization of differentially expressed transcript-derived fragments associated with 'floral bud distortion' in soybean. *J. Genet.* **95**, 787–799]

Introduction

At present, soybean is one of the important agricultural commodities with a steady increase in annual production. Soybean cultivation was negligible until 1970, particularly in India, thereafter it increased 37-fold since 1970, as compared to any other oilseed crop and stands next to groundnut in production. As plants are sessile, like other crops soybean is also prone to be attacked by various biotic and abiotic factors. Since last decade, floral bud distortion (FBD) has been found as an emerging threat for soybean production in central India (Jadhav *et al.* 2013). It is a peculiar disorder where the affected soybean plant fails to produce pods and does not senescence maturity even at the end of the season. Attempts to understand FBD is limited due to inadequate knowledge of its symptoms and causes. Hence, despite an upturn in published reports and evidence of losses, most researchers, extension workers and growers still remain unfamiliar with the disorder. The symptoms are unpredictable in their incidence and described globally with different names, namely no podding syndrome in India,

*For correspondence. E-mail: jpraveen26@yahoo.co.in.

Keywords. soybean; floral bud distortion; cDNA-decamer; cytology; *in silico* characterization; annotation; mapping.

a bud proliferation syndrome in USA (Lee *et al.* 2011) and pod set failure syndrome in Iran (Golnaraghi *et al.* 2004). Thus, it becomes a great concern for soybean growers in central India and other countries as well. According to the earlier reports, several biotic factors have been identified in the host leading to reduced pollen vigour (Subekti 2008), seed mass variants (Marr and Marshall 2006), floral abnormalities, sepal hypertrophy, virescence, phyllody, aborted reproductive organs (Pracros *et al.* 2006), enhanced vegetative growth (Singh and Bhatt 2013), premature flower abortion (Sugano *et al.* 2011), etc. Cytological examination of plant reproductive organs needs to be performed to understand their factual structural and functional disability associated with the disorder.

During successful plant development, there are numerous molecular events regulated by interacting with surrounding environment. A complex interaction in plant metabolic network is an outcome of fine regulation of plant genes singly or synergistically. The result of developmental alteration like FBD is projected as a partial or complete yield loss. Many developmental genes have been cloned and characterized to understand the mechanism of developmental abnormality in soybean (Xu *et al*. 2011; Hu *et al*. 2014; Huang *et al*. 2014; Wang *et al*. 2015). To determine the molecular alterations, different approaches have been used in different crops that are needed to explore here to understand the nature of FBD prevailing in soybean.

Currently, several molecular techniques, such as differential display reverse transcription-polymerase chain reaction (DD-RTPCR), representational difference analysis (RDA), serial analysis of gene expression (SAGE), suppression subtractive hybridization (SSH), ribotyping by random decamer primers and cDNA microarray are available for transcriptome analysis (Pagariya *et al.* 2011). By using these techniques, efforts were made to decipher the nature of various biotic and abiotic stresses and to identify genic fragments through electronic database searches. However, studies towards assessing the molecular response associated with the disorder are limited and hence efforts are being made to explore the insights of the FBD at molecular level. Recently, cDNA-decamer technique has been successfully used for determining differentially expressed TDFs in *Phalaenopsis orchids* (Chen *et al.* 2005), chickpea (Nimbalkar *et al.* 2006) and sugarcane (Kawar *et al.* 2010). It is proved as a cost-effective technique that provides information on complex phenotype reflecting changes in the abundance of RNAs under various conditions and does not require specialized expertise to handle as the other sophisticated technical activities. This method was found to be highly fruitful to highlight molecular insights of unknown plant biological aspects. Accordingly, the present investigation was aimed to assess the cytological behaviour of floral reproductive organs and molecular alterations associated with the disorder to identify molecular targets that were altered in symptomatic soybean plants. Similarly, the differentially expressed TDFs were characterized using *in silico* tools, namely BLAST homology, protein–protein interaction tool, gene prediction tool, prediction of subcellular location and mapping.

Materials and methods

Cytological attributes

The soybean genotype JS-335, commonly used in genetic improvement programme and commercially growing on more than 80% of the cropping area in the central India was used in this study. For cytological studies, five flowers of five symptomatic and asymptomatic plants of the same genotype were used for replicated experienced trails.

Pollen viability and germination assay

The flowers of symptomatic and asymptomatic plants of genotype JS-335 were collected at the R2 reproductive stage of the crop grown in the experimental field of Department of Agricultural Botany, Dr Panjabrao Deshmukh Agricultural University, Akola, India, during kharif season 2014. Samples were collected in the morning hours before anthesis, it was collected in Petri plates at 6–8°C while transport. Pollen viability was studied using the procedure by Johri and Vasil (1961) and pollen germination as per Firmage and Dafni (2001). Pollen was transferred onto microscope slides containing staining solution and covered immediately with a cover slip (Barrow 1983). After 20 min of incubation, slides containing pollens were observed under a compound microscope to record viability count in percentage.

Germination of pollen grains was carried out using standardized artificial pollen germination media (PGM) as per the method described by Firmage and Dafni (2001). Pollen grains were collected freshly and placed in hanging droplet (10 μL) of standardized PGM and incubate at room temperature for 24 h. A few drops of methylene blue (1–5 μL) were added to each spot in a square of carefully opened plate cover. Spots were examined under microscope to check the germination percentage. Pollen grains were considered germinated when the length of pollen tube was more than the diameter of the pollen grains. For each microscopic field, total number of pollen grains and the number of germinated grains were recorded.

Pollen morphology

Pollen morphology was studied in symptomatic and asymptomatic plants of JS-335 genotype at R2 stage. Fresh flowers were collected in the morning hours before anthesis and examined under scanning electron microscopy. The dehydration of flowers was done for 30 min each in a series of alcohol concentrations as 50, 60, 70, 80, 90 and 100%. After dehydration, the flowers were subjected to critical point drying (CPD) using liquid carbon dioxide with CPD7501 critical point dryer. After CPD, stigmas were placed on the aluminum stub having double adhesion tape and conducted with gold with JFC 1100 sputter. The stigmas were examined

under JSM 1100 JEOL scanning electron microscope at different magnifications.

Stigma receptivity assay

Replicated trials were made by evaluating five flowers from symptomatic and asymptomatic plants during the R1–R2 stage to assess stigma receptivity of symptomatic and asymptomatic soybean plants. The presence of peroxidase enzyme on the stigma surface reflects its receptivity. Therefore, the stigma was immersed into hydrogen peroxide (3%) and observed for bubbles and change in colour according to Dafni (1992). A colour change from light yellow to purple/brown indicated presence of peroxidases on receptive stigma. Stain intensity was used as an indicator of enzyme activity and classified as light, medium or dark.

Molecular attributes

RNA isolation and cDNA synthesis: Total RNA was isolated from three symptomatic and asymptomatic plant tissues (frozen bud, node and leaf tissues) at R5 stage using PureLink®RNA Mini Kit (Invitrogen, San Diego, USA) and stored in 50 μL of RNase free water. Reverse transcription of transcripts and second strand synthesis from 0.1 μg total RNAs was carried out using First Strand Synthesis kit (Thermo Scientific, Waltham, USA) and quantified by measuring OD at 260 nm. Normalization of synthesized cDNA was done prior to PCR profiling.

cDNA-decamere profiling: PCR amplification of quantified second-strand cDNA from each tissue of both symptomatic and asymptomatic soybean plants were achieved using 60 numbers of 10-mer decamer primers (OPD, OPF, OPA, OPI and OPH (Eurofins Genomics, Bengaluru, India). As much as 20 μL of PCR reaction mixture contained 10 ng of cDNA, 2 μL of 10× reaction buffer, 1 μL of RiboLock, 2 μL of 10 mM dNTP mix, 1 μL of 20 pmol primer and 2 units of M-MuLV reverse transcriptase. Amplifications were performed by a cycle of 5 min at 94°C followed by 39 cycles each of 1 min at 94°C, 1 min at 36°C, and 2 min at 72°C, and final extension of 15 min at 72°C. The PCR products were resolved on 1.8% agarose using TBE buffer. All the reactions were repeated thrice and consistently reproducible amplicons were scored and used for further studies.

Profile scoring and data analysis: Amplicon profile was scored and data was analysed based on the consensus results of three independent runs. Clearly resolved polymorphic bands (TDFs) of both symptomatic and asymptomatic plants were scored manually considering the presence/absence or differences in their intensity derived values (IDV). The differences in amplicons were assigned as upregulated and/or downregulated compared with IDV values of asymptomatic plant tissue considering as respective control. The IDV values derived using AlphaEaseFC (Genetic Technologies, Miami, USA) image processing software.

Amplicons derived from binary data in the form of 0 (for absence) and 1 (for presence) were used to generate a dendrogram. This was used to create group of the individuals according to Jaccard's coefficient for comparing sets of variables to distribute tissues under investigation.

Elution, validation and sequencing of differentially expressed TDFs: The individual differentially expressed TDFs were eluted from the agaros gel with sharp surgical blade without contaminating any fragment(s) in 30 μL of sterile double-distilled water using the QIAEX II gel extraction kit (Qiagen, Valencia, USA). Aliquot of 1 μL was used for amplifying individual TDF using same corresponding primer and analysed electrophoretically.

The nine sequences of the TDFs were studied using Chromas Lite 2.01 software. The sequence similarity analysis using BLAST homology against the publicly available nonredundant database (genes/ESTs/transcripts/protein) allowed their putative functional annotations (http://www.ncbi.nlm.nih.gov/Blast.cgi) (Altschul *et al.* 1997). Properly annotated four sequences were deposited at NCBI. Whereas, uncharacterized sequences were studied for their possible computational characterization of subcellular localization and predicted functions. Further, gene-specific relatedness were established with reference to FBD symptoms using already published reports to understand the pathways involved in such abnormal development of soybean flowers.

In silico protein interaction studies: Deciphering interactive links between proteins is needed to understand its role in multifaceted metabolic pathway(s). Reconstruction of complex pathways with predicted interaction networks based on available experimental data is becoming one of the most demanding requirements in the postgenomic era. This method can address the position of physically interacting proteins in pairs and identified the most likely motif involved in the interactions. Therefore, sequences annotated after BLAST homology were subjected to this study by protein–protein interaction tool-STRING as described by Franceschini *et al.* (2013). This is useful to discriminate between true and false interactions in a significant number of cases so as to generate information of target proteins. Here, virtual reconstruction of complete interacting networks can be determined to understand the possible role of protein(s) associated with FBD.

Subcellular protein localization: Subcellular localization of uncharacterized sequences was carried out using WoLFPSORT, a web-based tool. Further, this was used to obtain their possible role in the plant metabolism. Information generated for uncharacterized proteins will help to understand their possible functions and molecular alterations in FBD.

Physical mapping of TDFs: The available soybean databases (Phytozome, SoyBase and NCBI) were used to localize

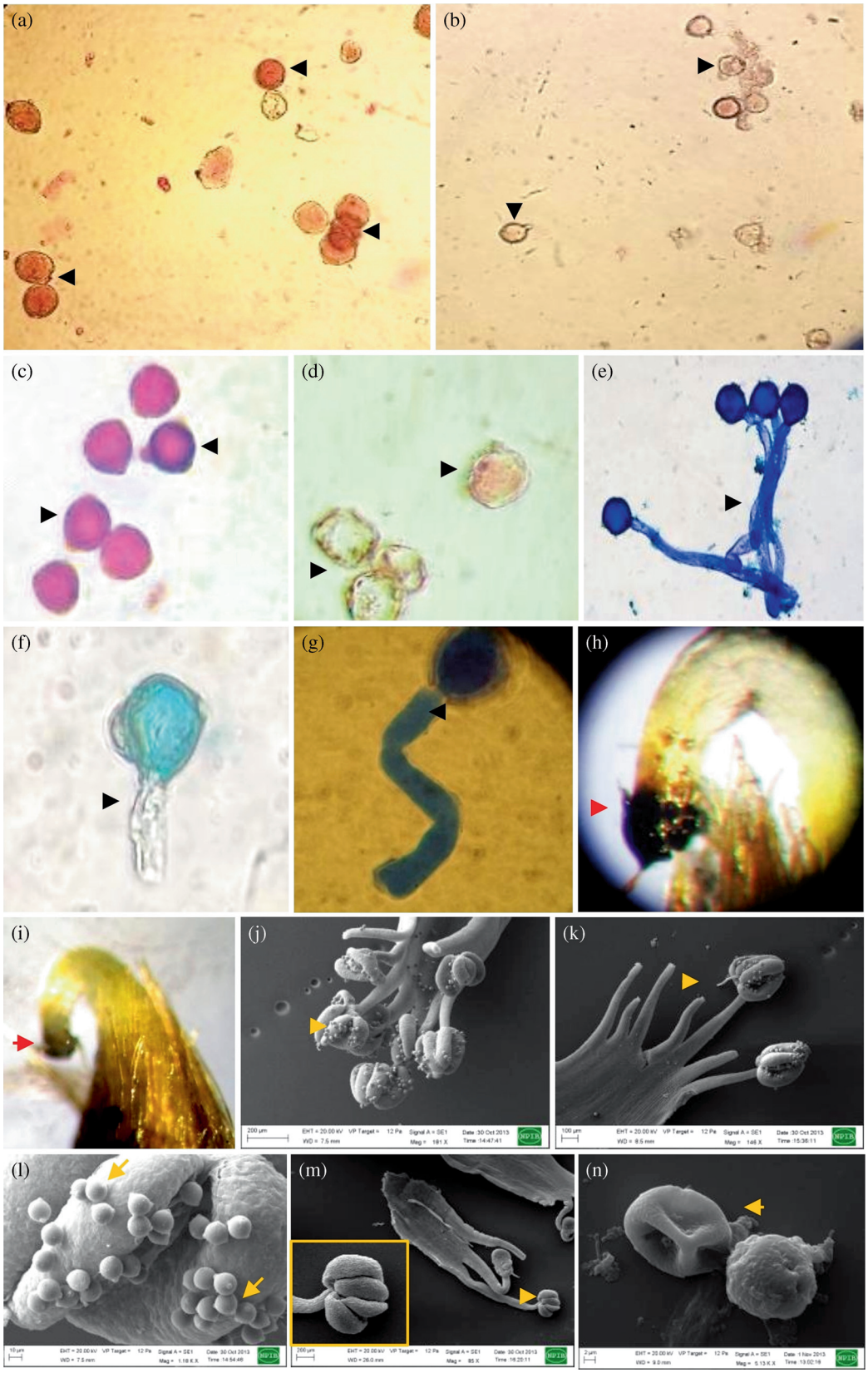

Figure 1. Cytological observations of floral organs in asymptomatic and symptomatic (FBD) soybean plant. Asymptomatic sample: pollen viability (a & c), pollen germination (e & g), stigma receptivity (h), pollen on anthers (j, k and l). Symptomatic sample: pollen viability (b & d), pollen germination (f), stigma receptivity (i), pollen on anthers (m), structural aberrations in pollens (n).

identified TDF sequences on virtual chromosomes of *Glycine max* to detect their distribution, relative position and abundance. The exact locations of TDFs were determined using MegaBLAST tool showing at least 80% identity (Soares-Cavalcanti *et al.* 2012).

Results

The FBD: symptoms and prevalence

FBD is a peculiar disorder limiting soybean yield in central India. The conspicuous morphological symptoms recorded were the plants showing prolonged vegetative phase (stay green) even after R8 stage without pod. The symptomatic plants found randomly distributed in the field and failed to produce pods leading to complete yield loss. Neither we can predict the occurrence in the field nor identify the symptomatic plants at an early stage. The symptoms produced did not resemble with any of the documented diseases or pest of soybean. The soybean plants showed a complex set of visible symptoms associated with extended vegetative phase, stay green plants and FBD leads to reduced pods and resulting in yield loss. The roving survey of the soybean growing regions of central India showed yield loss ranged from 5–50% during two succeeding seasons. In case of genotypewise average incidence for two succeeding seasons, *Kh*-2010 and *Kh*-2011, revealed Samrat as a most vulnerable to the FBD with an incidence of 30%, followed by JS 93-05 (21%). Genotype JS-335 showed moderate vulnerability with 13.2% incidence and 13% for Sonia Gold (Jadhav *et al*. 2013). However, during the following years, highest incidence was recorded in genotype JS-335 (90%) followed by JS-93-05 (58.8%) (Jadhav *et al*. 2013). The genotype JS-335 was therefore used for further cytological and molecular experimentations.

Cytological behaviour of floral reproductive organs

Pollen morphology, viability and germinability: The results showed that there was a significant difference in the number of pollens, morphology and functionality between symptomatic and asymptomatic plants. Pollens of symptomatic plants were reduced in number, size, shape, viability and germinability. The pollens of symptomatic plants were shrunk, transparent with less cytoplasm and thicker exine wall. Whereas, pollens in asymptomatic plants exhibited remarkably no morphological abnormality having dense cytoplasm with prominently stained nucleolus at the centre (figure 1). The width of anther was increased by 1.4-fold with few numbers of pollens recorded in symptomatic plants. The reduced pollen viability of 33.98% was recorded in symptomatic plant while 89.93% of viable pollens found in asymptomatic plant. The pollen germination of 17.62% and 38.78% were recorded in symptomatic plant after 24 and 48 h, respectively. However, 41.85% and 59.94% pollen germinability was recorded in asymptomatic plants after 24 and 48 h, respectively (unpublished observations) (table 1).

Table 1. Per cent pollen viability and pollen germination in asymptomatic and symptomatic plants.

Staining solution	Asymptomatic (mean (±SD))	Symptomatic (mean (±SD))
Pollen viability (%)	89.93 (±1.04)	33.98 (±0.65)
Pollen germination (%) after 24 h	41.85 (±0.74)	17.62 (±0.75)
Pollen germination (%) after 48 h	59.94 (±1.06)	38.78 (±1.15)

Values in the table are mean values of five replicates of each experiment.

Stigma receptivity: The repeated experiments showed the presence of peroxidase activity showing reddish brown colour on the stigmas of both the plants. Hence, stigma found receptive in symptomatic and asymptomatic plants (figure 1).

Molecular studies

cDNA synthesis and profiling of differentially expressed TDFs: The quantified cDNA of three tissues of symptomatic and asymptomatic plants (R2–R3) was profiled using 60 decamer primers. Altogether 197 scorable amplicons were generated from 60 decamer primers and the transcript size varied from 162 to 1130 bp. The binary data was generated scoring clearly resolved amplicons and dendrogram using Jaccard's coefficient. Different tissues of symptomatic and asymptomatic plants were distributed in two different clusters (A and B). However, leaf tissue of symptomatic plant grouped in the cluster B representing asymptomatic plant. This may be due to no differential changes in leaves of symptomatic and asymptomatic plant.

Of the 197 amplicons, 171 were monomorphic and 26 found differentially regulated. Among the differentially expressed amplicons, 15 were found completely polymorphic and 11 showed differences in their IDVs revealing either upregulation or downregulation. The IDVs of the amplicons were scored for intensity of the amplicon using AlphaEaseFC software and were assigned upregulation and downregulation by comparing with their respective controls, i.e. asymptomatic plant.

Sequence similarity search/BLAST: The PCR amplified products were gel purified and were confirmed by PCR and subjected to sequencing. Of the total 26 differentially expressed TDFs, nine were found reproducible when screened on 10 different symptomatic and asymptomatic plants. The post sequencing data was processed using the sequence analysis tools (Chromas Lite 2.01 software). The processed sequences of nine TDFs were analysed for their homology. This was carriedout against the database publicly available (http://www.ncbi.nlm.nih.gov/Blast.cgi) as per the method described by Altschul *et al.* (1997). Annotations describing details of sequences after a homology search of the sequences are presented in table 2. Among the nine sequences, properly annotated four sequences were deposited in NCBI database with accession numbers, namely KR864892, KR827485, KR827486 and KR820243.

Table 2. List of TDFs and their accession number features based on sequences homology studies.

Name assigned	Regulation pattern	Homology hits	Organism	NCBI accession no.	Definition (in this study)	Subcellular localization
Seq1.FBD.212	Up	Predicted: auxin response factor 9-like (LOC100799088), mRNA	*G. max*	KR820243	*G. max* cultivar JS-335 auxin response factor 9-like protein partial mRNA	–
Seq2.FBD.304	Down	Predicted: uncharacterized LOC100815325 (LOC100815325), transcript variant X1, mRNA	*G. max*	KR827486	*G. max* cultivar JS-335, partial 5′UTR region of uncharacterized transcript variant X1, mRNA	Cytosol
Seq3.FBD.477	Down	Predicted: FHA domain-containing protein At4g14490-like (LOC102667282), mRNA	*G. max*	KR864892	*G. max* cultivar JS-335 FHA domain-containing protein like mRNA, partial cds	Plasma membrane
Seq4.FBD.300	Up	Predicted: probable isoaspartyl peptidase/L-asparaginase 2-like (LOC101492649), mRNA	*C. arietinum*	–	–	–
Seq5.FBD.400	Up	Hypothetical protein (MTR_4g090180) mRNA, complete cds	*M. truncatula*	–	–	Nuclear
Seq6.FBD.400	Down	Hypothetical protein (PHAVU_005G068000g) mRNA, complete cds	*P. vulgaris*	–	–	Nuclear
Seq7.FBD.400	Up	Predicted: pentatricopeptide repeat-containing protein At3g22690-like (LOC100798950), mRNA	*G. max*	–	–	–
Seq8.FBD.250	Down	Hypothetical protein (PHAVU_002G071200g) mRNA, complete cds	*P. vulgaris*	–	–	Cytosol
Seq9.FBD.311	Down	Predicted: uncharacterized LOC102667978, mRNA	*G. max*	KR827485	*G. max* cultivar JS-335 unnamed protein	Cytosol

In silico protein interactome (four characterized proteins): Possible functions of the differentially expressed TDFs are depicted in table 2. After annotation, the sequences were analysed for their interaction link between other cellular protein(s) using *in silico* protein interaction tool (Szklarczyk *et al.* 2014; http://string-db.org/). Reconstruction of complex interactions by using available predictions and experimental data are becoming one of the most demanding needs in the postgenomic era. This method directly addresses the position of physically interacting protein in pairs and identifies the most likely sequence motifs involved in the interactions. In this experiment, two characterized TDFs were analysed using this tool, namely *G. max* auxin response factor 9-like gene (*ARF9*) and *G. max* forkhead-associated (FHA) domain-containing protein.

- The ARF9 (KR820243) is a transcriptional factor that binds specifically to the DNA sequence at 5′-TGTCTC-3′ located in the auxin-responsive promoter elements (AuxREs). This is involved in the overall plant development, phase transition from vegetative to reproductive and environmental signalling pathways. *In silico* interactome studies showed its interaction with other transcription factors like ARF6, TIR1 and MP (figure 2a). Further, the trancription factor ARF9 is found distributed in the genome of *G. max* on chromosomes 1, 3, 7 and 18 (table 3).
- FHA domain-containing protein (KR864892), also known as DAWDLE (DDL) is phosphoprotein-binding domains involved in protein–protein interactions of signal transduction pathways. Correspondingly, direct and/or indirectly (in combination with other interacting proteins) responsible for altered morphology in plants. *In silico* interesting studies showed DDL interacts with 'Dicer-like 1' protein, which is expressed in flowers, seeds, ovule integuments, inflorescence and floral meristems, stigma of flowers and embryo. Other interacting protein 'hyponastic leaves 1' (HYL1) is characterized by shorter plant height, delayed flowering, leaf hyponasty, reduced fertility, decreased root growth rate and an altered root gravitropic response. It also exhibits less sensitivity to auxin and cytokinin. Among other interacting proteins, few are with unknown functions, but majority have known functions like, DNA/RNA/protein/ion binding, splicing or mRNA maturation, PTGS in circadian clock and flowering time genes, protein folding and pathogen response (figure 2b).

However, unnamed protein (KR827485) and uncharacterized transcript variant X1 (KR82748) did not show any interaction. Based on literature, it is assumed that alterations in above described gene expression may lead to cause major morphological alterations similar to FBD.

Subcellular localization and functional characterization

Numerous experiments to determine protein localization have been performed to date (Horton *et al.* 2007). Bilipid membranes divide eukaryotic cells into various types of

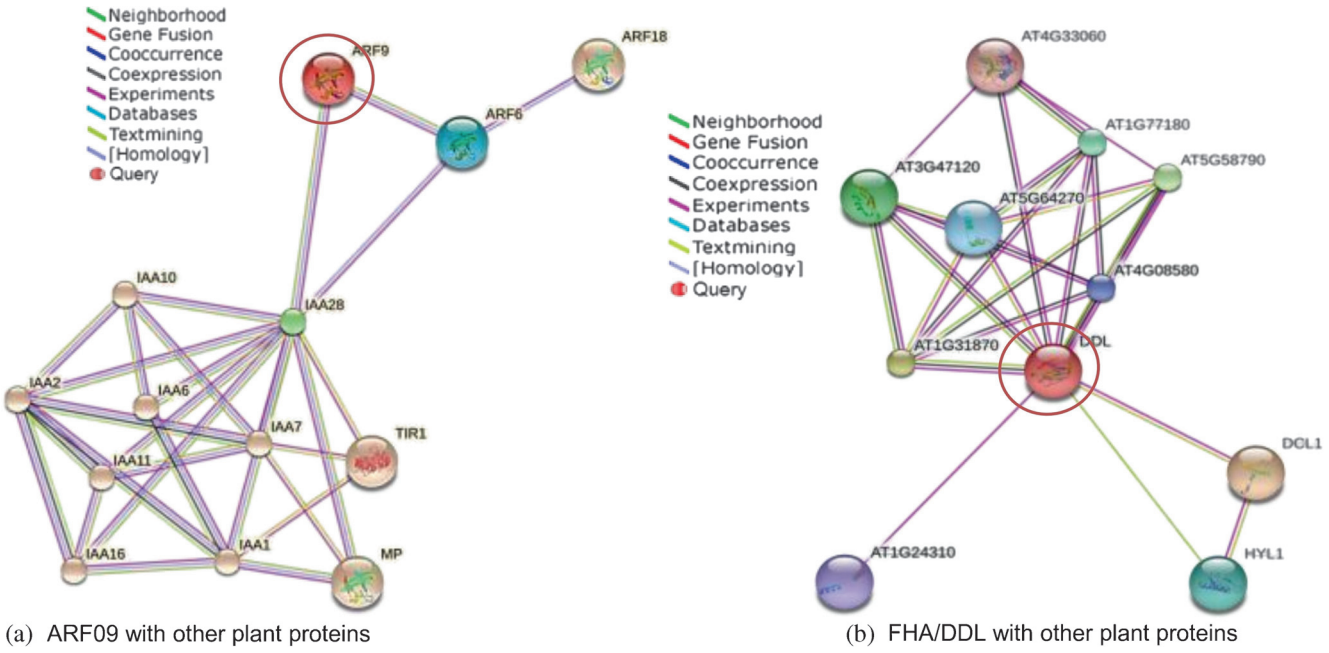

Figure 2. Protein interaction networking of ARF09 (a) and FHA/DDL (b) with other plant proteins.

Table 3. List of ARF 9-like transcription factors and their distribution in *G. max* L. genome.

Symbol	Chromosome	Genomic nucleotide accession	Start position on accession	End position on accession	Orientation	Exon count
LOC100820503	3	NC_016090.1	47281238	47285829	Plus	14
LOC100780060	18	NC_016105.1	48724216	48729843	Plus	13
LOC100803911	1	NC_016088.1	33301170	33305526	Minus	14
LOC100799088	7	NC_016094.1	15910708	15916243	Plus	13
LOC100779003	3	NC_016090.1	22232910	22237542	Plus	14

organelles containing characteristic proteins and performing specialized functions. Thus, subcellular localization provides important information about protein's function.

In the present investigation, TDFs were screened to understand their subcellular location and possible role in the plant metabolisms using WoLF PSORT. Table 1 represents possible subcellular locations and their functions of proteins derived from TDFs.

Genomewide identification of all TDFs by physical mapping

The MegaBLAST tool was used to ascertain the location of TDFs in the genome (Soares-Cavalcanti *et al.* 2012). The soybean genome (NCBI database) was used for anchoring identified TDF sequences (seq. 1 to 9 from table 2) on chromosomes of *G. max*. This revealed anchorage pattern, distribution and abundance on chromosomes of the soybean genome (figure 3). While detailed results generated during mapping are depicted in table 4.

With respect to genomic distribution of the nine sequences anchorage clusters could be seen on all chromosomes except chromosomes 9 and 16 (figure 3). Pairs of duplicated sequence hits on different chromosomes are common in all sequences except seq. 2 in this experiment. Seq. 2 is found uncharacterized and may be studied further for its better understanding and possible role in FBD.

Discussion

Morphological and microscopic studies

FBD is a disorder, serving major yield loss in the growing region of soybean. This is a condition where the soybean fails to produce pods and does not sense the end of the season. FBD leads to low or total yield loss in symptomatic plants and deterioration of seed quality, if developed. Green plants show slow harvest as compared to asymptomatic field and this leads to a loss of a season. In fact, symptomatic plant samples are randomly distributed in the field and often growers could not recognize the problem until it is too late to save the crop. Further, former could not predict the occurrence in field condition/location. For experimental study purposes one could not preserve the collected plants/samples from the field.

Present investigation showed evidence of morphological, cytobiochemical and molecular behaviour of FBD in soybean (*G. max*). Similar symptoms have been described

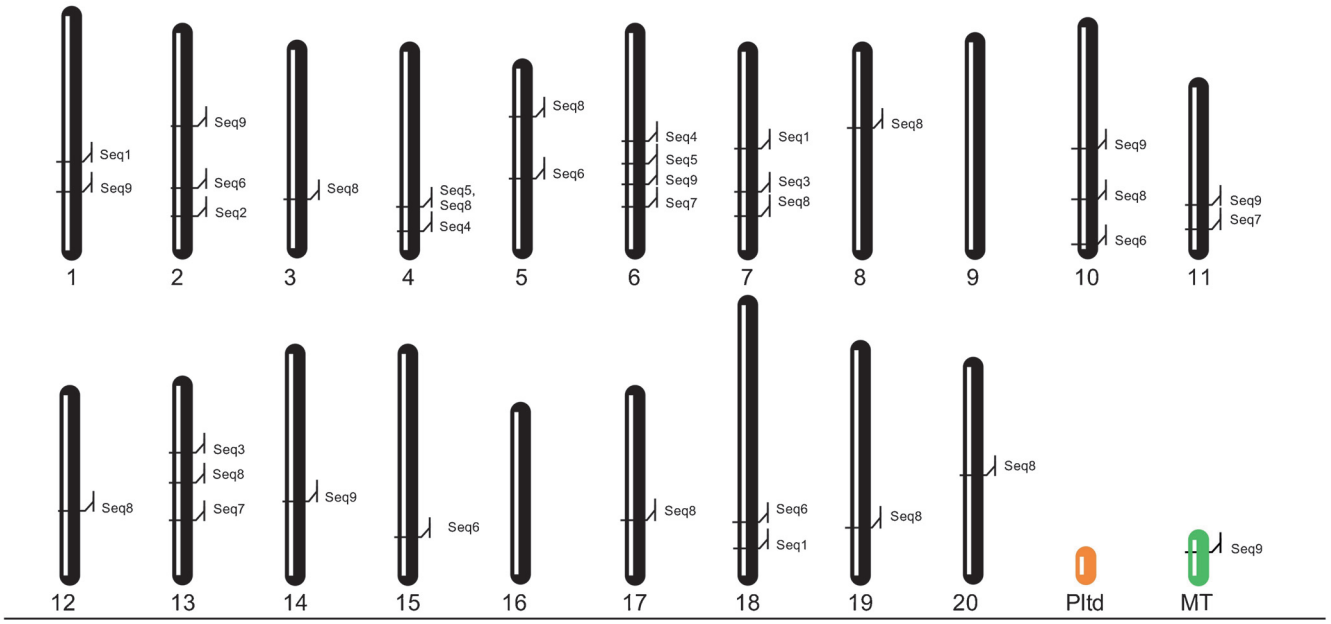

Figure 3. Computationally generated physical map of TDF sequences against soybean genome. Schematic representation of sequences 1 to 9 (see table 2 for description) generated in this experiment and that were anchored in soybean genome upon BLAST similarity tool at NCBI database.

earlier globally in different appellations, namely pod set failure in Iran (Golnaraghi *et al.* 2004); no podding syndrome in India and bud proliferation syndrome in US (Lee *et al.* 2011). Jadhav *et al.* (2013) reported cytological behaviour of symptomatic soybean plants and characterized the symptoms as 'floral bud distortion'. Depending on the location, many different factors have been associated with FBD, including viruses, phytoplasma, soybean aphids, thrips, stink bugs, leafhoppers, bean leaf beetles and Cercospora leaf blight, etc. (Jadhav *et al.* 2013).

Cytological behaviour of pollen revealed significant differences in symptomatic and asymptomatic plants. The reduced number of pollen and distorted in shape were found in symptomatic plants. Contrary, asymptomatic plant was round in shape. According to earlier reports, abnormalities in pollen development may occur because of abiotic factors (Koti *et al.* 2005) and/or biotic factors (Subekti 2008) which play contributory role and also reported for synergistic effect. Silva *et al.* (2011) reported pollen viability based on staining ability and *in vitro* pollen germination. Earlier researchers used multiple stains like acetocarmine (Ling *et al.* 2012), potassium iodine iodide (Djanaguiraman *et al.* 2013) and vital dye solution (Johri and Vasil 1961). All the methods described in methodology proved their importance in the measurement of pollen viability percentage. In the present investigation, the only difference was found in pollen staining ability among the tests.

Concur with the present findings, the description of abnormal pollens has been reported by Koti *et al.* (2005). The difference in size and shape of pollen was noticed under contrasting character and reported shrinkage in pollen grains under stressed condition (Koti *et al.* 2005).

In vitro pollen germination was studied to assess germinability and growth of pollen tube under controlled conditions by Heslop-Harrison (1992). Germination success in sucrose medium depends on the humidity to which the pollen grains were exposed prior to the germination test and on the pollen age (Heslop-Harrison 1992). The sucrose medium contains essential elements in its formulation for pollen tube germination such as boron and calcium nitrate. These elements maintain the extracellular ion flow and the intracellular of protein and calcium gradient that are necessary for pollen tube development (Holdaway-Clarke and Hepler 2003). The highest pollen germination percentage was obtained in normal plant than the stressed (Koti *et al.* 2005).

Stigma receptivity is a crucial stage in the maturation of the flower that greatly influence: (i) rate of selfpollination; (ii) the success of pollination at different stages of flower development; (iii) relative importance of various pollinators; and (iv) interference between the functions of male and female organelle (Knox 1984). The presence of peroxidase enzyme reflects the stigma receptivity. Peroxidases generally catalyses the breakdown of hydrogen peroxide to yield highly oxidizing intermediates which oxidises a variety of organic and inorganic reducing substrates (McInnis *et al.* 2006).

According to earlier reports, the difference in size and shape of pollen was reported shrinkage in pollen grains in development of symptomatic plant by Srinivasan *et al.* (1999) and Nayyar *et al.* (2005). Ling *et al.* (2012) reported the interspecific hybrid of *Nicotiana tabacum* × *N. glauca* was not able to set seed because of empty and shriveled pollens in hybrid plants and was incapable of germination.

Table 4. Locations of TDFs on chromosomes of *G. max* (L) by virtual karyotyping.

Chromosome no.	Map element	Hits	Score	*E* value
	Seq1.FBD.212			
1	NW_003722731 Glycine max chromosome 1 genomic scaffold, V1.0 GLYMAchr_01, whole genome shotgun sequence	1	91.6	8e-17
7	NW_003722737 Glycine max chromosome 7 genomic scaffold, V1.0 GLYMAchr_07, whole genome shotgun sequence	2	418	3e-115
18	NW_003722748 Glycine max chromosome 18 genomic scaffold, V1.0 GLYMAchr_18, whole genome shotgun sequence	2	259	2e-67
	Seq2.FBD.304			
2	NW_003722732 Glycine max chromosome 2 genomic scaffold, V1.0 GLYMAchr_02, whole genome shotgun sequence	3	484	3e-135
	Seq3.FBD.477			
7	NW_003722737 Glycine max chromosome 7 genomic scaffold, V1.0 GLYMAchr_07, whole genome shotgun sequence	1	73.4	3e-11
13	NW_003722743 Glycine max chromosome 13 genomic scaffold, V1.0 GLYMAchr_13, whole genome shotgun sequence	1	78.8	8e-13
	Seq4.FBD.300			
4	NW_003722734 Glycine max chromosome 4 genomic scaffold, V1.0 GLYMAchr_04, whole genome shotgun sequence	1	505	2e-141
6	NW_003722736 Glycine max chromosome 6 genomic scaffold, V1.0 GLYMAchr_06, whole genome shotgun sequence	1	342	2e-92
	Seq5.FBD.400			
4	NW_003722734 Glycine max chromosome 4 genomic scaffold, V1.0 GLYMAchr_04, whole genome shotgun sequence	1	361	5e-98
6	NW_003722736 Glycine max chromosome 6 genomic scaffold, V1.0 GLYMAchr_06, whole genome shotgun sequence	1	243	2e-62
	Seq6.FBD.400			
2	NW_003722732 Glycine max chromosome 2 genomic scaffold, V1.0 GLYMAchr_02, whole genome shotgun sequence	1	35.6	5.7
5	NW_003722735 Glycine max chromosome 5 genomic scaffold, V1.0 GLYMAchr_05, whole genome shotgun sequence	1	41.0	0.13
10	NW_003722740 Glycine max chromosome 10 genomic scaffold, V1.0 GLYMAchr_10, whole genome shotgun sequence	1	37.4	1.6
15	NW_003722745 Glycine max chromosome 15 genomic scaffold, V1.0 GLYMAchr_15, whole genome shotgun sequence	3	41.0	0.13
18	NW_003722748 Glycine max chromosome 18 genomic scaffold, V1.0 GLYMAchr_18, whole genome shotgun sequence	1	37.4	1.6
	Seq7.FBD.400			
6	NW_003722736 Glycine max chromosome 6 genomic scaffold, V1.0 GLYMAchr_06, whole genome shotgun sequence	1	35.6	5.5
11	NW_003722741 Glycine max chromosome 11 genomic scaffold, V1.0 GLYMAchr_11, whole genome shotgun sequence	2	37.4	1.6
13	NW_003722743 Glycine max chromosome 13 genomic scaffold, V1.0 GLYMAchr_13, whole genome shotgun sequence	1	35.6	5.5

Table 4 (*contd*)

Chromosome no.	Map element	Hits	Score	*E* value
	Seq8.FBD.250			
3	NW_003722733 Glycine max chromosome 3 genomic scaffold, V1.0 GLYMAchr_03, whole genome shotgun sequence	3	33.7	9.3
4	NW_003722734 Glycine max chromosome 4 genomic scaffold, V1.0 GLYMAchr_04, whole genome shotgun sequence	1	33.7	9.3
5	NW_003722735 Glycine max chromosome 5 genomic scaffold, V1.0 GLYMAchr_05, whole genome shotgun sequence	1	33.7	9.3
6	NW_003722736 Glycine max chromosome 6 genomic scaffold, V1.0 GLYMAchr_06, whole genome shotgun sequence	1	33.7	9.3
7	NW_003722737 Glycine max chromosome 7 genomic scaffold, V1.0 GLYMAchr_07, whole genome shotgun sequence	1	33.7	9.3
8	NW_003722738 Glycine max chromosome 8 genomic scaffold, V1.0 GLYMAchr_08, whole genome shotgun sequence	**3**	33.7	9.3
10	NW_003722740 Glycine max chromosome 10 genomic scaffold, V1.0 GLYMAchr_10, whole genome shotgun sequence	1	33.7	9.3
12	NW_003722742 Glycine max chromosome 12 genomic scaffold, V1.0 GLYMAchr_12, whole genome shotgun sequence	1	33.7	9.3
13	NW_003722743 Glycine max chromosome 13 genomic scaffold, V1.0 GLYMAchr_13, whole genome shotgun sequence	**3**	33.7	9.3
17	NW_003722747 Glycine max chromosome 17 genomic scaffold, V1.0 GLYMAchr_17, whole genome shotgun sequence	**2**	33.7	9.3
19	NW_003722749 Glycine max chromosome 19 genomic scaffold, V1.0 GLYMAchr_19, whole genome shotgun sequence	1	33.7	9.3
20	NW_003722750 Glycine max chromosome 20 genomic scaffold, V1.0 GLYMAchr_20, whole genome shotgun sequence	**2**	33.7	9.3
	Seq9.FBD.311			
1	NW_003722731 Glycine max chromosome 1 genomic scaffold, V1.0 GLYMAchr_01, whole genome shotgun sequence	**2**	37.4	1.6
2	NW_003722732 Glycine max chromosome 2 genomic scaffold, V1.0 GLYMAchr_02, whole genome shotgun sequence	**2**	37.4	1.6
6	NW_003722736 Glycine max chromosome 6 genomic scaffold, V1.0 GLYMAchr_06, whole genome shotgun sequence	1	35.6	5.4
10	NW_003722740 Glycine max chromosome 10 genomic scaffold, V1.0 GLYMAchr_10, whole genome shotgun sequence	1	37.4	1.6
11	NW_003722741 Glycine max chromosome 11 genomic scaffold, V1.0 GLYMAchr_11, whole genome shotgun sequence	1	37.4	1.6
14	NW_003722744 Glycine max chromosome 14 genomic scaffold, V1.0 GLYMAchr_14, whole genome shotgun sequence	1	37.4	1.6
Not mapped	NW_003723495	1	35.6	5.4

Molecular attributes

Chen *et al.* (2005), Nimbalkar *et al.* (2006), Ghag *et al.* (2014) and Phanchaisri *et al.* (2012) described cDNA-RAPD technique and demonstrated its importance in the identification of differentially expressed TDFs between stress and non-stressed plants. Correspondingly, identification of molecular alterations in the plants showing distorted floral buds are

needed to understand the mechanism of the disorder. This information will be helpful in understand the disorder in detail. In the present study, differential gene expression studies using oligo-decamer primers revealed a profile on agarose gel. Binary data of this profile were used to generate tissue-wise clusters in this study. The distribution of tissues in two clusters, each from symptomatic and asymptomatic. In this cluster, leaf tissue of symptomatic group was found placed in asymptomatic cluster. Looking at the morphological studies in this experiment, leaves were not showing significant morphological alterations in FBD. Hence, this may be due to comparatively less alterations in leaves than that of a pod and the node of symptomatic sample.

Despite of advantages for using cDNA-RAPD in developing laboratories, there are some limitations when compared with recently introduced next-genaration sequencing based RNA-Seq approaches. Experiments using cDNA-RAPD are time consuming and generate relatively limited data of diffrentially expressed elements. Also, there is less coverage of transcriptome in cDNA RAPD than that of RNA-Seq methods which provides a comprehensive picture of differential regulation among the tissues under experimentation. Understanding the comprehensive picture of transcriptome is essential for interpreting the functional elements of the genome and revealing the molecular constituents of cells and tissues, and also for understanding developmental alterations (Wang *et al.* 2009).

Identification and functional categorization of sequences

Auxin response factors (ARFs): Transcription factors (TFs) are important target in understanding the regulation of plant responses to environmental stimuli. The sequence KR820243 showed partial homology with ARF 9-like gene. The ARF TFs bind with specificity to TGTCTC-containing AuxREs found in the regulatory promoter region of primary/early auxin response genes and mediate responses to the plant hormone auxin (Ulmasov *et al.* 1997a, b). Ultimately, these play a critical role in growth responses throughout the development of a plant such as tropisms, apical dominance and root initiation, and responses on a cellular level, such as cell extension, division and differentiation (Hagen and Guilfoyle 2002). It has been found that number of ARF gene members in *G. max* L. are 23 whereas that of *Arabidopsis* is 23 and 25 in rice (Ulmasov *et al.* 1999; Wang *et al.* 2007).

The ARF genes are represented by a large multigene family in plants. Numerous sequences that were upregulated or downregulated by auxin have already been described (Abel and Theologis 1996; Sitbon and Perrot-Rechenmann 1997; Guilfoyle and Hagen 2007) and are categorized in three major classes (*Aux/IAA*s, *SAUR*s and *GH3*s). The majority of ARF proteins consist of three typical modular domains: an amino-terminal DNA-binding domain (DBD), a carboxy-terminal dimerization domain (CTD), and a middle domain (MD) (Hagen and Guilfoyle 2002; Tiwari *et al.* 2003; Guilfoyle and Hagen 2007). An ARF protein contains a DNA-binding domain in the N-terminal region. A carboxyterminal dimerization was a protein interaction domain that mediates the homodimerization and heterodimerization, which seems like the domains III and IV founding in the C terminus of Aux/IAAs. A MD may function as either an activation domain (AD) or repression domain (RD) (Ulmasov *et al.* 1997a, b; Ulmasov *et al.* 1999), both of which mediate cellular response by activating or repressing downstream gene expression (Finet *et al.* 2013). According to earlier reports, glutamine-rich middle region of ARF proteins found as activator in different ARF families namely, ARF5, ARF6, ARF7, ARF8 and ARF19 (Tiwari *et al.* 2001; Wang *et al.* 2005a, b). However, in contrast, ARF1, ARF2, ARF3, ARF4, and ARF9 contain a proline-rich and/or serine-rich regions, or lack a Gln-rich region, and act as transcriptional repressors (Ulmasov *et al.* 1999; Tiwari *et al.* 2003).

FHA domain-containing protein

The FHA domain-containing protein is the first identified in a group of forkhead TFs, but found in a wide variety of proteins from both prokaryotes and eukaryotes. DAWDLE (DDL), is a FHA domain-containing protein in *Arabidopsis*, acts in the biogenesis of miRNAs and endogenous siRNAs (Yu *et al.* 2008). It is a phosphoprotein-binding domain involved in protein–protein interactions of signal transduction pathways. Further, FHA domains may bind phosphothreonine, phosphoserine and sometimes phosphotyrosine, distinguishing them from other well-studied phosphoprotein-binding domains (Mahajan *et al.* 2005). In plants, the FHA domain is part of a protein that localizes to the plasma membrane and participates in the regulation of receptor-like protein kinase signalling pathways. In other eukaryotes, many proteins containing an FHA domain are found in the nucleus and involved in DNA repair, cell cycle arrest or pre-mRNA processing (Li *et al.* 2000). Further, Li *et al.* (2000) showed a functional FHA domain consists of 120–140 amino acid residues, which is significantly larger than the sequence motif previously described. Although, FHA domains do not exhibit extensive sequence similarity, they share similar secondary and tertiary structures, featuring a sandwich of two antiparallel (beta)-sheets (Li *et al.* 2000).

During this experiment *in silico* interactome studies showed FHA-containing DDL interacts with 'Dicer-like 1' protein, which is expressed in flowers, seeds, ovule integuments, inflorescence and floral meristems, stigma of flowers and embryo. Other interacting protein 'hyponastic leaves 1′ (HYL1) is characterized for shorter plant height, delayed flowering, leaf hyponasty, reduced fertility, decreased rate of root growth, and an altered root gravitropic response. It also exhibits less sensitivity to auxin and cytokinin. Among other interacting proteins, some are with unknown functions, but the majority have known functions, namely DNA/RNA/protein/ion binding, splicing or mRNA maturation, PTGS in circadian clock and flowering time genes, protein folding and pathogen response.

Another report by Ahn *et al.* (2013), FHA domain is involved in protein–protein interaction by recognizing a phosphothreonine epitope on target proteins. In *Arabidopsis*, the forkhead-associated domain 2 (AtFHA2) mainly localized in the nucleus and reduced fertility during reproductive stage. Specifically found involvement in plant organ development, particularly stamen filament elongation but not having a role in the development of female parts in flower. These results correlate with the present findings of abnormal male reproductive parts in FBD.

Certainly, this study identifies the deferentially expressed transcripts, however to confirm their role, additional studies are required. The genes which are altered in the symptomatic plant and their cause(s) are unknown. Further studies should address these targeted gene(s) associated with FBD.

Acknowledgements

We sincerely thank the Department of Atomic Energy (DAE), Board of Research in Nuclear Sciences (BRNS), Government of India, Mumbai, India for providing financial support (grant no. 2013/37B/44/BRNS/1904).

References

Abel S. and Theologis A. 1996 Early genes and auxin action. *Plant Physiol.* **111**, 9–17.

Ahn E. R., Cho H. K. and Pai H. S. 2013 The forkhead-associated domain 2 (FHA2) in Arabidopsis plays a role in plant fertility by regulating stamen development. *Planta* **237**, 1015–1023.

Altschul S. F., Madden T. L. and Schaffer A. A. 1997 Gapped BLAST and PSI-BLAST: a new generation of protein database search programs. *Nucleic Acids Res.* **25**, 3389–3402.

Barrow J. R. 1983 Comparisons among pollen viability measurement methods in cotton. *Crop Sci.* **23**, 734–736.

Chen Y. H., Tsai Y. J., Huang J. Z. and Chen F. C. 2005 Transcription analysis of peloric mutants of Phalaenopsis orchids derived from tissue culture. *Cell Res.* **15**, 639–657.

Dafni A. 1992 *Pollination ecology: a practical approach*. Oxford University Press, Oxford, UK.

Djanaguiraman M., Prasad P. V. V., Boyle D. L. and Schapaugh W. T. 2013 Soybean pollen anatomy, viability and pod set under high temperature stress. *J. Agron. Crop. Sci.* **199**, 171–177.

Finet C., Berne-Dedieu A., Scutt C. P. and Marletaz F. 2013 Evolution of the ARF gene family in land plants: old domains, new tricks. *Mol. Biol. Evol.* **30**, 45–56.

Firmage D. H. and Dafni A. 2001 Field tests for pollen viability; a comparative approach. *Acta Hortic.* **561**, 87–94.

Franceschini A., Szklarczyk D., Frankild S., Kuhn M., Simonovic M., Roth A. and Jensen L. J. 2013 STRING v9. 1: protein–protein interaction networks, with increased coverage and integration. *Nucleic Acids Res.* **41**, D808–D815.

Ghag S. B., Shekhawat U. K. and Ganapathi T. R. 2014 Characterization of Fusarium wilt resistant somaclonal variants of banana cv. Rasthali by cDNA-RAPD. *Mol. Biol. Rep.* **41**, 7929–7935.

Golnaraghi A. R., Shahraeen N., Pourrahim R., Farzadfar S. and Ghasemi A. 2004 Occurrence and relative incidence of viruses infecting soybeans in Iran. *Plant Disease.* **88**, 1069–1074.

Guilfoyle T. J. and Hagen G. 2007 Auxin response factors. *Curr. Opin. Plant. Biol.* **10**, 453–460.

Hagen G. and Guilfoyle T. 2002 Auxin-responsive gene expression: genes, promoters and regulatory factors. *Plant Mol. Biol.* **49**, 373–385.

Heslop-Harrison J. S. 1992 Cytological techniques to assess pollen quality. In *Sexual plant reproduction*, pp. 41–48. Springer Berlin Heidelberg.

Holdaway-Clarke T. L. and Hepler P. K. 2003 Control of pollen tube growth: role of ion gradients and fluxes. *New Phytol.* **159**, 539–563.

Horton P., Park K. J., Obayashi T., Fujita N., Harada H., Adams-Collier C. J. and Nakai K. 2007 WoLF PSORT: protein localization predictor. *Nucleic Acids Res.* **35**, W585–W587.

Hu Q., Jin Y., Shi H. and Yang W. 2014 GmFLD a soybean homolog of the autonomous pathway gene FLOWERING LOCUS D, promotes flowering in *Arabidopsis thaliana*. *BMC Plant Biol.* **14**, 263.

Huang F., Xu G., Chi Y., Liu H., Xue Q., Zhao T. *et al.* 2014 A soybean MADS-box protein modulates floral organ numbers, petal identity and sterility. *BMC Plant Biol.* **14**, 89.

Jadhav P. V., Mane S. S., Nandanwar R. S., Kale P. B., Dudhare M. S., Moharil M. P. and Dani R. G. 2013 Floral bud distortion in soybean and incidence in Central India. *Egy. J. Biol.* **15**, 59–65.

Johri B. M. and Vasil I. K. 1961 Physiology of Pollen. *Bot. Rev.* **27(3)**, 318–381.

Kawar P. G., Pagariya M. C., Dixit G. B. and Prasad D. T. 2010 Identification and isolation of SCGS phytoplasma-specific fragments by riboprofiling and development of specific diagnostic tool. *J. Plant Biochem. Biot.* **19**, 185–194.

Knox R. B. 1984 Pollen-pistil interactions. In: *Cellular interactions*, pp. 508–608. Springer Berlin Heidelberg.

Koti S., Reddy K. R., Reddy V. R. and Zhao D. 2005 Interactive effects of carbon dioxide, temperature, and ultraviolet-B radiation on soybean (*Glycine max* L.) flower and pollen morphology, pollen production, germination and tube lengths. *J. Exp. Bot.* **56**, 725–736.

Lee I. M., Bottner-Parker K. D., Zhao Y., Villalobos W. and Moreira L. 2011 'Candidatus Phytoplasma costaricanum' a novel phytoplasma associated with an emerging disease in soybean (*Glycine max*). *Int. J. Syst. Evol. Micr.* **61**, 2822–2826.

Li J., Lee G. L., Doren S. R. V. and Walker J. C. 2000 The FHA domain mediates phosphoprotein interactions. *J. Cell Sci.* **113**, 4143–4149.

Ling H. Y., Edwards A. M., Gantier M. P., DeBoer K. D., Neale A. D., Hamill J. D. and Walmsley A. M. 2012 An interspecific Nicotiana hybrid as a useful and cost-effective platform for production of animal vaccines. *PLoS One* **7**, e35688.

Mahajan A., Yuan C., Pike B. L., Heierhorst J., Chang C. F. and Tsai M. D. 2005 FHA domain-ligand interactions: importance of integrating chemical and biological approaches. *J. Am. Chem. Soc.* **127**, 14572–14573.

Marr D. L. and Marshall M. L. 2006 The role of fungal pathogens in flower size and seed mass variation in three species of *Hydrophyllum* (Hydrophyllaceae). *Am. J. Bot.* **93**, 389–398.

McInnis S. M., Emery D. C., Porter R., Desikan R., Hancock J. T. and Hiscock S. J. 2006 The role of stigma peroxidases in flowering plants: insights from further characterization of a stigma-specific peroxidase (SSP) from *Senecio squalidus* (Asteraceae). *J. Exp. Bot.* **57**, 1835–1846.

Nayyar H., Bains T. and Kumar S. 2005 Low temperature induced floral abortion in chickpea: relationship to abscisic acid and cryoprotectants in reproductive organs. *Env. Exp. Bot.* **53**, 39–47.

Nimbalkar S. B., Harsulkar A. M., Giri A. P., Sainani M. N., Franceschi V. and Gupta V. S. 2006 Differentially expressed gene transcripts in roots of resistant and susceptible chickpea plant (*Cicer arietinum*) upon *Fusarium oxysporum* infection. *Physiol. Mol. Plant. Pathol.* **668**, 176–188.

Pagariya M. C., Harikrishnan M., Kulkarni P. A., Devarumath R. M. and Kawar P. G. 2011 Physio-biochemical analysis and transcript profiling of *Saccharum officinarum* L. submitted to salt stress. *Acta Physiol. Planta* **33**, 1411–1424.

Phanchaisri B., Samsang N., Yu L., Singkarat S. and Anuntalabhochai S. 2012 Expression of OsSPY and 14-3-3 genes involved in plant height variations of ion-beam-induced KDML 105 rice mutants. *Mutat. Res. Fund. Mol. Mech. Mut.* **734**, 56–61.

Pracros P., Renaudin J., Eveillard S., Mouras A. and Hernould M. 2006 Tomato flower abnormalities induced by stolburphytoplasma infection are associated with changes of expression of floral development genes. *Mol. Plant Microbe. Interact.* **19**, 62–68.

Silva N., Mendes-Bonato A. B., Sales J. G. C. and Pagliarini M. S 2011 Meiotic behaviour and pollen viability in *Moringa oleifera* (Moringaceae) cultivated in southern Brazil. *Genet. Mol. Res.* **10**, 1728–1732.

Singh A. K. and Bhatt B. P. 2013 Occurrence of phytoplasma phyllody and witches' broom disease of Faba bean in Bihar. *J. Env. Bio.* **34**, 837–840.

Sitbon F. and Perrot-Rechenmann C. 1997 Expression of auxin-regulated genes. *Physiol. Plant.* **100**, 443–455.

Soares-Cavalcanti N. M., Belarmino L. C., Kido E. A., Pandolfi V., Marcelino-Guimarães F. C., Rodrigues F. A. *et al.* 2012 Overall picture of expressed heat shock factors in *Glycine max*, Lotus japonicus and Medicago truncatula. *Genet. Mol. Biol.* **35**, 247–259.

Srinivasan A., Saxena N. P. and Johansen C. 1999 Cold tolerance during early reproductive growth of chickpea (*Cicer arietinum* L.), genetic variation in gamete development and function. *Field Crops Res.* **60**, 209–222.

Subekti N. A. 2008 The effects of disease on plant reproduction as basis for breeding for disease resistance. In Proceedings of the scientific seminar and annual meeting of the regional commissioner PEI PFI XIX South Sulawesi 5 November pp. 167–180. Komisariat Daerah Sulawesi Selatan, Indonesia.

Sugano J., Melzer M., Pant A., Radovich T., Fukuda S. and Migita S. 2011 Field evaluations of Tomato Yellow Leaf Curl Virus Resistant Varieties for Commercial Production. College of Tropical Agriculture and Human resources. PD-78. http://scholarspace.manoa.hawaii.edu/bitstream/10125/33260/1/PD-78.pdf.

Szklarczyk D., Franceschini A., Wyder S., Forslund K., Heller D., Huerta-Cepas J. *et al.* 2014 STRING v10: protein–protein interaction networks, integrated over the tree of life. *Nucleic Acids Res.* **1**, 1–6.

Tiwari S. B., Hagen G. and Guilfoyle T. 2003 The roles of auxin response factor domains in auxin-responsive transcription. *Plant Cell* **15**, 533–543.

Tiwari S. B., Wang X. J., Hagen G. and Guilfoyle T. J. 2001 Aux/IAA proteins are active repressors, and their stability and activity are modulated by auxin. *Plant Cell* **13**, 2809–2822.

Ulmasov T., Hagen G. and Guilfoyle T. J. 1997a ARF1, a transcription factor that binds to auxin response elements. *Science* **276**, 1865–1868.

Ulmasov T., Murfett J., Hagen G. and Guilfoyle T. J. 1997b Aux/IAA proteins repress expression of reporter genes containing natural and highly active synthetic auxin response elements. *Plant Cell* **9**, 1963–1971.

Ulmasov T., Hagen G. and Guilfoyle T. J. 1999 Dimerization and DNA binding of auxin response factors. *Plant J.* **19**, 309–319.

Wang D., Pei K., Fu Y., Sun Z., Li S., Liu H. *et al.* 2007 Genome-wide analysis of the auxin response factors (ARF) gene family in rice (*Oryza sativa*). *Gene* **394**, 13–24.

Wang J. W., Wang L. J., Mao Y. B., Cai W. J., Xue H. W. and Chen X. Y. 2005a Control of root cap formation by microRNA-targeted Auxin Response Factors in Arabidopsis. *The Plant Cell* **17**, 2204–2216.

Wang M., Xu X., Zhang X., Sun S., Wu C., Hou W. *et al.* 2015 Functional analysis of GmCPDs and investigation of their roles in flowering. *PLoS One* **10**, e0118476.

Wang S., Tiwari S. B., Hagen G. and Guilfoyle T. J. 2005b AUXIN RESPONSE FACTOR7 restores the expression of auxin-responsive genes in mutant Arabidopsis leaf mesophy11 protoplasts. *Plant Cell* **17**, 1979–1993.

Wang Z., Gerstein M. and Snyder M. 2009 RNA-Seq: a revolutionary tool for transcriptomics. *Nat. Rev. Genet.* **10**, 57–63.

Xu F., Meng T., Li P., Yu Y., Cui Y., Wang Y. *et al.* 2011 A soybean dual-specificity kinase, GmSARK, and its Arabidopsis homolog, AtSARK, regulate leaf senescence through synergistic actions of auxin and ethylene. *Plant Physiol.* **157**, 2131–2153.

Yu B., Bi L., Zheng B., Ji L., Chevalier D., Agarwal M. *et al.* 2008 The FHA domain proteins DAWDLE in Arabidopsis and SNIP1 in humans act in small RNA biogenesis. *Proc. Natl. Acad. Sci. USA* **105**, 10073–10078.

Received 20 June 2015, in final revised form 29 December 2015; accepted 15 February 2016
Unedited version published online: 18 February 2016
Final version published online: 18 October 2016

Corresponding editor: JITENDRA P. KHURANA